

Tapered Bladed of Vertical Axis Wind Turbine for Powering Street Lights in Urban Areas in Indonesia with Wind Speed of 2-4 m/s

Maria Fransisca Soetanto^{1*}, Yackob Astor², Singgih Satrio Wibowo¹, Syaiful³, Muhammad Rizki Zuhri¹, Mochammad Luthfi¹

¹Department of Mechanical Engineering,
Politeknik Negeri Bandung, Jl Gegerkalong Hilir, West Bandung, 40559, INDONESIA

²Department of Civil Engineering,
Politeknik Negeri Bandung, Jl Gegerkalong Hilir, West Bandung, 40559, INDONESIA

³Department of Mechanical Engineering,
Universitas Diponegoro, Jl. Prof. Soedarto, SH., Semarang, 50275, INDONESIA

*Corresponding Author: mariasoetanto@polban.ac.id

DOI: <https://doi.org/10.30880/ijie.2024.16.06.022>

Article Info

Received: 12 August 2024

Accepted: 9 October 2024

Available online: 5 November 2024

Keywords

Tapered blade, VAWT, CFD, wind speed, street light

Abstract

This paper presents the development of a vertical axis wind turbine (VAWT) with blades in the form of a taper curved profile using caps on the top and bottom of the turbine. The blade development was carried out based on numerical calculations using the Computational Fluid Dynamic (CFD) method using ANSYS Workbench 2018 software by comparing the use of conventional blades. The flow pattern that occurs around the turbine shows that the tapered curved blade design has a more distributed vortex formation pattern compared to conventional curved blades, and the turbulence that occurs at top speed ratio, or TSR = 1.0 is still in the turbine blade area, which means the wind turbine in this research has a larger speed range compared to previous research. The experimental results of the characteristics of the wind turbine prototype parameters obtained the maximum coefficient of power, $C_{p-max} = 0,14$ at TSR 1.11, and was able to turn on LED streetlight and was able to fully charge the battery within 4 hours. The experiment results of this study are presented in the form of bar chart of C_{p-max} , compared with the Savonius results of previous studies, at almost the same TSR. It is obtained that the C_p of this wind turbine works with C_p 18.9 % greater than the previous results. So, this wind turbine is suitable for use in urban areas in Indonesia which have wind speeds of 2 – 4 m/s.

1. Introduction

Around 20 percent of Indonesia's population still lack access to electricity [1]. Indonesia's electrical generation is heavily dependent on fossil fuels, especially coal, but Indonesia's supply of fossil fuels estimated will run out in the next 42 years and the coal-fired power plants (CFPP) cause environmental pollution problems, as well as impacts on public health [2] [3]. So, the national energy policy revision set a target of 23% of renewables in 2025, or 255 MW of capacity of wind power plans while until 2020 has only installed around 135 MW [4], even then these wind turbines are located on islands that have high wind speed characteristics, 6-7 m/s [5], such as those found on Selayar island and Janeponto in South Sulawesi [6], Sukabumi – West Java [7]; while the wind speeds characteristic in the majority of urban and rural areas, such as on the island of Java and other islands with densely populated, are low category, 1-4 m/s [8] based on the distribution map of onshore and offshore wind speeds as

This is an open access article under the CC BY-NC-SA 4.0 license.



seen in Fig. 1, so these wind turbines are not suitable for applied. Thus, the development of wind energy in Indonesia is still a national challenge.

From Fig. 1, it can be seen that the wind speed on Indonesia's onshore is dominated by green color, with a rate of $V = 1-2$ m/s and green light color, with a rate of $V = 3-4$ m/s. The minimum wind speed required to spin the blade of a wind turbine is 5 m/s, so the mean annual wind speed in Indonesia is low. Therefore, it requires research to optimize the wind energy potential, especially regarding the type of blade that can spin at a lower wind speed [9].

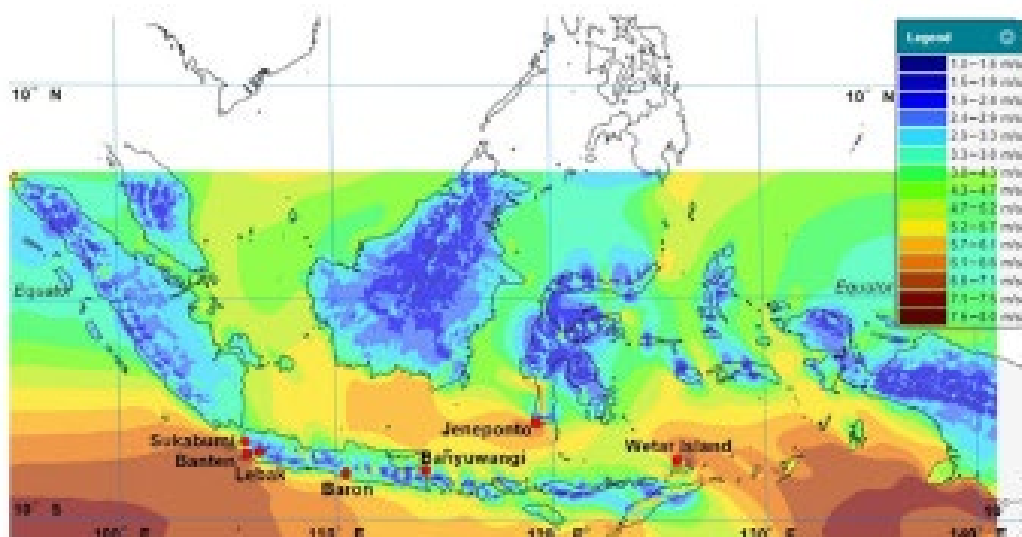


Fig. 1 Map of Indonesia's wind speed measured at 11 locations by the Indonesian Center for Maritime and Geological Development Research [8]

Due to their simplicity and ease of manufacturing, Savonius-rotor type vertical axis wind turbines (VAWT) are still considered one of the most attractive solutions [10] [11] [12]. Besides, Savonius VAWTs are well suited to such environments due to their inherent axisymmetric design, which can reduce loads on the turbine tower to reduce material costs and enable urban areas with low wind potential to be supplied with clean electric power. These benefits are necessary for the installation and continued operation of cheap small-scale wind turbines [13] [14] [15]. In this paper, a vertical axis wind turbine (VAWT) with 3 blades in the form of a taper curved profile using caps on the top and bottom of the turbine is developed that can be used as driving energy for street lighting and has been adapted to the wind speed conditions of most Indonesia's onshore islands. This research was carried out numerically and experimentally.

Numerical calculations are carried out to obtain the characteristics of the aerodynamic parameters of the air flow around the turbine, such as flow patterns, pressure distribution, vortex formation, and determining the coefficient values of aerodynamic forces, where the results obtained will be compared with the use of conventional blade. This numerical calculation is carried out using the Computational Fluid Dynamic (CFD) method using ANSYS Workbench 2018. Next, a VAWT prototype is made according to the design and then tested experimentally to obtain performance parameters at the test location. With this type of VAWT, the wind's kinetic energy is converted into mechanical energy through the rotation of the taper-tip wind turbine blades, and then the rotation of the wind turbine will be forwarded to the generator through gear transmission and will be converted into electrical energy by the generator. The electricity produced by the generator will be stored in the battery. The process of storing and distributing electrical energy will be regulated by the charger controller.

This paper discusses the streamlined patterns and pressure distribution that occur in the space between blades to generate aerodynamic forces, compared to conventional VAWT. This paper also discusses the lift force coefficient and drag coefficient as functions of the tip speed ratio (TSR).

2. Literature Review

The following are some reviews of previous studies related to this paper: Menet, J.-L., & Rezende, T. de [16] developed a Savonius Wind Turbine with Double Wind Tunnels that could generate output voltage but had a limited range of wind angle (60 to 75 degrees of wind angle). Sanusi et al. [17] presented a blade combination of a Savonius wind turbine where the conventional circle-shaped model is combined with the one of a concave

elliptical model. It improves the performance of the power coefficient maximum (C_{pmax}) up to 11% compared to the conventional blade at $TSR = 0.79$, but there is a drop-in performance in the use of endplates linking shaft.

Nemati [18] combined Two-bladed Savonius with a three-bladed straight Darrieus. It can function at low wind speeds and low TSR, but the geometry of the turbine is too complex to produce. Pallotta et al. [19] combined a two-bladed Savonius with a three-bladed helical Darrieus. The turbine can be self-started; the cutting speed is less than Darrieus, but it needs a high wind speed and is also too complex to produce. Lee & Zhao [20] stated that the primary investment for a wind farm comes from the area and turbine cost, the initial investment was around USD 0.02/kWh. Therefore, further research is needed to reduce the cost of wind farm energy. Mishra et al. [21] studied a novel concept of testing a Savonius wind turbine with dimple structures on its blades and investigating their effect on the turbine's efficiency. The study also deals with the experimental validation of the effect of using a converging ducted structure with single-stage and double-stage configurations of the Savonius wind turbine. The result proves that the power coefficient increases with the addition of dimple structures on the blades.

Belmili et al. [22] presented a conventional Savonius VAWT double blade equipped with a photovoltaic panel and a storage system (battery) that can be used both for remote areas and for building integration on the Algerian East-West Highway for lighting and/or petrol station electrical equipment supply. This paper also examines numerically using SolidWork software but does not explain how this VAWT works at what wind speed.

The flow field and aerodynamic performance of a Vertical Axis Swirling Savonius Turbine (SST) was studied using the CFD package of ANSYS CFX by Abdullah Al-Faruk, Ahmad Sharifian [23]. However, the lack of detailed descriptions of the flow field around the swirling Savonius turbine inhibits a complete understanding of the performance of VAWT. M. Zemamou, M. Aggour, and A. Toumi [24] compared several results of published articles on the performance of new designs of Savonius rotors by optimizing different geometric designs and concluded that the addition of some sets of new designs can achieve a 27,3 percent improvement in the performance coefficient compared to the conventional Savonius VAWT.

B. D. Altan and G.S. Gultekin [25] determined that the power coefficient values of Savonius wind turbines with additional exterior designs have been increased up to 0.520 levels, compared to 0,400 levels with interior designs. However, turbines with exterior design additions occupy a larger space, which can lead to a wind blockage effect in collective uses such as wind farms. Deda Altan, B., and Gungor, A. [26], Investigated the turbine performance of dual Savonius wind turbines by placing a flat plate deflector in front of the turbines and obtained that the power coefficient increased by 42% in the flat plate dual Savonius turbine system compared to the single Savonius wind turbine. The study conducted numerical analysis using the CFD program ANSYS Fluent.

From the results of previous research, the savonius type VAWT was widely developed with blade modifications, such as the use of tunnel-shaped blade by Promdee, C. & Photong, C. [27], as well as with the addition of accessories, such as adding a slide to the blade by Shouman, M.R., et al. [28], or the implementation of a tubercle around the Savonius VAWT by Sridhar, S., et al. [29], all proved to improve the performance of the turbine, but unfortunately all such designs did not fit the conditions of urban and rural Indonesian areas with low wind speeds.

3. Methodology

3.1 Model Description

The numerical calculation as the first stage of this study begins with determining the computational domain and meshing. A 3D-Simulation was carried out with the assumption that the fluid is an incompressible and steady-state, and were carried out using a laminar model for an inlet velocity of 2 m/s ($Re = 821540$) and a Spalart Allmaras model was applied in this study because this model has the ability to decreases the complexity of the problem and the overall simulation time [30]. A SIMPLE algorithm was used to solve velocity and pressure coupling by discretizing the equation. A second-order method for solving gradient term and upwind scheme for divergence term. The convergence criteria for the continuity, momentum, and energy equations, respectively, must meet the conditions of less than 10^{-5} , 10^{-5} , and 10^{-8} . The equations of aerodynamic forces are [31]:

Lift coefficient:

$$C_l = \frac{2L}{qA} \quad (1)$$

Drag coefficient:

$$C_d = \frac{2D}{qA} \quad (2)$$

Where: L = Lift, D= Drag, q = dynamic pressure, and A = surface area. Formation Equation used in the numerical simulation were:

$$\frac{\partial \tilde{v}}{\partial t} + u_j \frac{\partial \tilde{v}}{\partial x_j} = C_{b1}[1 - f_{t2}]\tilde{S}\tilde{v} + \frac{1}{\sigma}\{\nabla \cdot [(v + \tilde{v})\nabla \tilde{v}] + C_{b2}|\nabla \tilde{v}|^2\} - \left[C_{w1}f_w - \frac{C_{b1}}{\kappa^2}f_{t2}\right]\left(\frac{\tilde{v}}{d}\right)^2 + f_{t1}\Delta U^2 \quad (3)$$

With:

$$\tilde{S} \equiv S + \frac{\tilde{v}}{\kappa^2 d^2} f_{v2}, \quad f_{v2} = 1 - \frac{\chi}{1 + \chi f_{v1}} \quad (4)$$

$$f_w = g \left[\frac{1 + C_{w3}^6}{g^6 + C_{w3}^6} \right]^{\frac{1}{6}}$$

$$g = r + C_{w2} \frac{r^6 - r}{\tilde{v}} \quad (5)$$

$$r \equiv \frac{\tilde{S} \kappa^2 d^2}{\omega_t^2}$$

$$f_{t1} = C_{t1} g_t \exp\left(-C_{t2} \frac{\omega_t^2}{\Delta U^2} [d^2 + g_t^2 d_t^2]\right) \quad (6)$$

$$f_{t2} = C_{t3} \exp(-C_{t4} \chi^2) \quad (7)$$

$$S = \sqrt{2\Omega_{ij}\Omega_{ij}} \quad (8)$$

$$\Omega_{ij} = \frac{1}{2} \left(\frac{\partial u_i}{\partial x_j} - \frac{\partial u_j}{\partial x_i} \right) \quad (9)$$

Fig. 2 provides a simple flow chart of the work process of this study. The power coefficient is calculated numerically from the aerodynamic forces of this VAWT simulation study and will be compared with the results of the research conducted by N.M. Ali, A.K. Abdulhasan, S. Aljabair [32] for single stage Savonius wind turbine.

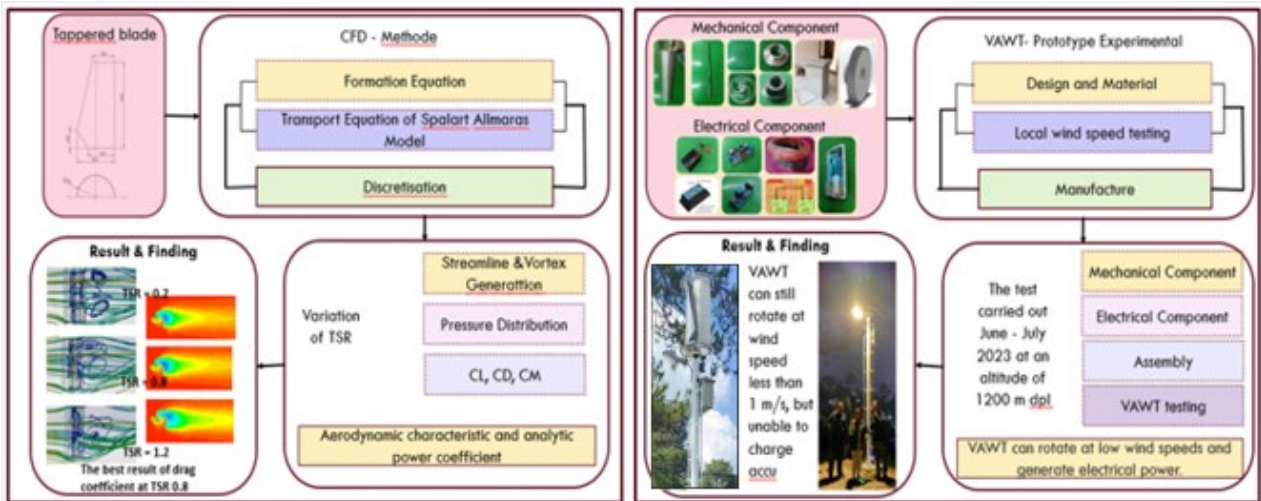


Fig. 2 Working process flowchart

3.2 Prototype VAWT and Experimental Testing

A VAWT prototype with a scale of 1:1 was subsequently made according to the numerical simulation geometry design. Mechanical and electrical components are also adapted to the design requirements in Table 1.

4. Results & Discussions

4.1 Numerical Simulation Calculation

Fig. 3 (a) shows the geometry of the Savonius-type, three-bladed, tapered-shaped VAWT of this study in an arranged volume that shapes a block with the center of the VaWT on the axis (0,0,0). In this simulation, air flows into the inlet with a velocity of 2 m/s. The positive x-axis direction is defined as a outlet with a pressure outlet type with a distance of 3.5 m from the axis so that the flow is possible to fully developed. The other sides of the surface are defined as Symmetry, and the VAWT is determined as Wall. The next process is the creation of the mesh shown in Fig. 3. (b). Fig. 4 shows the streamline of the flow around the VAWT of this research. Seeing at TSR

0.2 a vortex is formed at the upper end and the lower end at the back of the VAWT, then the vortex formation area will be wider, and the two vortices are closer to each other on TSR 0.4 and the area is increasingly enlarged and approaching each other at TS R 0.8. This means that the drag force as a turbine propeller increases with the addition of the TSR and reaches the optimum value at 0.8 TSR.

Table 1 Specification of VAWT prototype

| No | Component | Dimension (mm) | Specification |
|----|---------------------------|------------------|-------------------------------------|
| 1 | Pillar | Ø165 x 5000 | Mild steel ASTM A53 |
| 2 | VAWT blade | Ø 400 x 1000 | Aluminum |
| 3 | Turbine Shaft | Ø25 x 1700 | ST 37 ASTM A29 |
| 4 | VAWT flange | Ø97 x 37 | ST 37 |
| 5 | VAWT top and bottom cover | Ø500 x 6 | Acrylic |
| 6 | Top bearing mount | Ø105 x 33 | Aluminum |
| 7 | Bottom bearing mount | Ø105 x 23 | Aluminum |
| 8 | Bearing | Ø52 x 17 | Tapered Roller Bearing ISO 355:2019 |
| 9 | VAWT gear | Ø 232,50 x 25 | Spur gear M =1,5 Z =153 |
| 10 | Generator gear | Ø 93 x 25 | Spur gear M =1,5 Z = 60 |
| 11 | Box panel | 300 x 200 x 400 | Mild steel |
| 12 | Accumulator | 150 x100 x 180 | 10A 12v |
| 13 | Street lamp | 300 x 150 x 100 | LED DC 30 watt |
| 14 | Lamp Pole | Ø20 x 400 | Aluminum |
| 15 | Generator | Ø78 x 130 | 12V 1A,1000 rpm |
| 16 | Sensor LDR | 50 x 80 | DC |
| 17 | bolts | M5 x 10 | ISO 4762 |
| 18 | bolts | M6 x 30 | ISO 4017 |
| 19 | bolts | M10 x 30 | ISO 4762 |
| 20 | Hex nuts | M5 5mm thickness | ISO 4035 |
| 21 | Rivet | 4 mm | ISO 15973 |
| 22 | Anchor bolts | M 22 x 60 | JIS G3112-1995 |

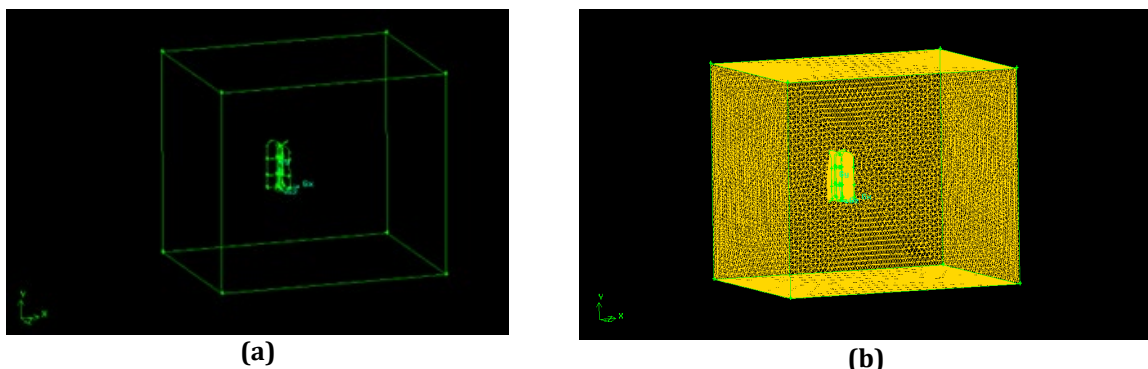


Fig. 3 (a) VAWT in control volume and its boundaries; and (b) Mesh generated

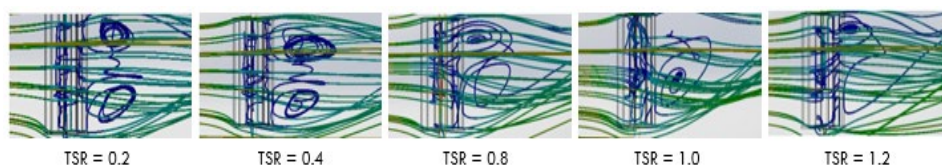


Fig. 4 Flow pattern and vortex creation on TSR variations

From Fig. 5, it can be explained that the blade's turbine area, which is expressed through a gradation of red to yellow color, has a greater pressure, with a pressure range of 0.336 Pa to 2.95 Pa. Meanwhile, the blade area, which is represented by a yellow to green color gradation, has a lower pressure, with a pressure range from -2.72 Pa to 0.336 Pa; thus, the turbine blade will move from blade 1 to blade 2 and blade 3 and rotate in a counterclockwise direction. Fig. 6 shows the velocity distribution in vector form based on tip speed ratio (TSR) variation: 0.2, 0.4, 0.6, 0.8, and 1.0 indicates that the vortex formation occurs in the space between blades 1 and blade 2, and reaches the middle of the area at TSR = 0.6, then increases towards the leading edge of the blade or towards the shaft at TSR = 0.8, and finally fills the entire area at TSR = 1.0. The formation of a vortex indicates the addition of drag, which in VAWT is required to rotate the turbine, so it can be analyzed that the maximum drag is obtained at TSR = 1.0. The results of the simulation of the drag coefficient and the analytical calculation of power-coefficients are shown in Table 2. The calculations at wind speed $v = 2 \text{ m/s}$ and TASN = 0.8 obtained a power coefficient of 0.195, while the results of previous studies for a conventional three-blade savonius wind turbine with a single stage at the same speed, obtain a power factor of 0.15 [32]. This means the three-bladed VAWT design with the tapered type can optimize power by 30%.

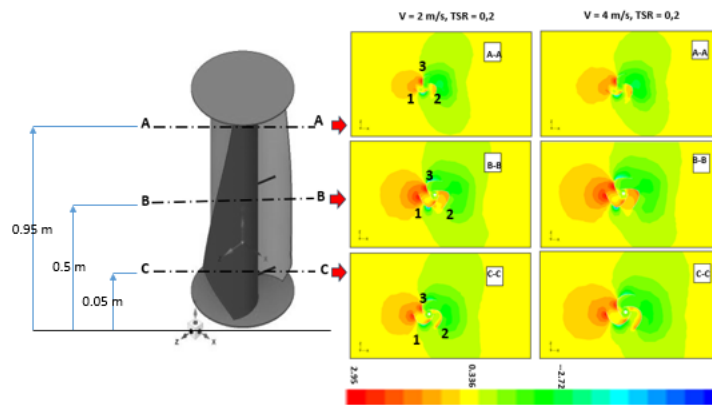


Fig. 5 VAWT current study with pressure distribution at 3 cutting planes for TSR = 0.2 at $V = 2 \text{ m/s}$ and $V = 4 \text{ m/s}$

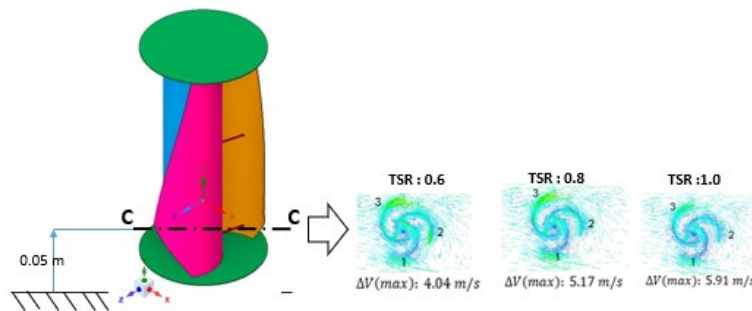


Fig. 6 VAWT current study with velocity vector on the cutting planes C-C with various TSR

Table 2 Specification of VAWT prototype

| Tip Speed Ratio, TSR | Rotation, ω (rad/s) | Drag Coefficient, C_d | Drag, D (N) | Torque, T (Nm) | Power, P (watt) | Power Coefficient, C_p |
|----------------------|----------------------------|-------------------------|-------------|----------------|-----------------|--------------------------|
| 0.2 | 2.667 | 0.2469 | 4.559 | 1.368 | 3.647 | 0.049 |
| 0.4 | 5.33 | 0.2456 | 4.535 | 1.360 | 7.255 | 0.098 |
| 0.6 | 8 | 0.2448 | 4.520 | 1,356 | 10.847 | 0.147 |
| 0.8 | 10.667 | 0.2433 | 4.492 | 1.348 | 14.375 | 0.195 |
| 1.0 | 13.33 | 0.2437 | 4.499 | 1.350 | 17.977 | 0.214 |
| 1.2 | 14.2 | 0.223 | 4.102 | 1.230 | 17.466 | 0.20 |

4.2 Experimental Testing

The VAWT installation site of this research is located on Cihanjuang Rahayu street at a height of 1200 mdpl with the majority of the population's subsistence as a flower farmer. Measurements were carried out in the morning

and evening during the months of June and July 2023. The results of the measurement obtained an average speed of 2.2 m/s, not much different from the input value of wind speed given in the numerical simulation.

The next test is a test on the VAWT without a load of a LED light or battery charging to know the voltage and current that comes out of the generator. The results are shown in Table 3. Based on the load-free test results in Table 3, the average voltage generated by the generator is 9.2 volts and the current generated is 0.16 Ampere, so it is possible to know the charge time of the battery with a capacity of 10 Ah is 62.5 hours.

Table 3 Specification of VAWT prototype

| Test Data Unloaded | | | |
|-----------------------|------------------------|---------------------------|-------------------------|
| Wind speed, v (m/s) | Rotation Turbine (RPM) | Current, I out (Ampere) | Voltage, V out (Volt) |
| 1.16 | 57.6 | 0.09 | 4.3 |
| 2.6 | 110.9 | 0.14 | 9.6 |
| 2.71 | 147.6 | 0.16 | 10 |
| 2.79 | 143.9 | 0.25 | 10.3 |
| 3.2 | 179.4 | 0.19 | 11.8 |

Further testing is carried out on the VAWT with a load of LED light to determine the voltage and current that comes out of the accumulator with the results as in Table 4. From the data measurement of wind speed and turbine rotation speed calculations obtained the calculation of power estimates and power coefficients on the VAWT with the load of the light. Table 5 displays the calculation data for turbine power and electric power generated by the VAWT. Fig. 7 (a). show the results of VAWT production this research results after assembly and ready for testing and Fig. 7 (b). show evidence of the VAWD test has managed to turn on the LED light, so that the result of this research can be used as an alternative to the production of street lighting in urban and rural areas in Indonesia or elsewhere that has characteristics of low wind speed. The numerical calculation results of this research are displayed in the form of a CP curve for the specified TSR variations, as seen in Fig. 8 (a) which is compared with the conventional Savonius [32]. It can be seen that the maximum Cp value resulting from this study is 18.9% greater than conventional. Apart from that, the peak of the curve that moves from TSR = 0.8 to TSR = 1.0 will provide a wider speed range, which means the performance of the wind turbine will increase. Furthermore, the results of numerical calculations and experiments in this study, compared with previous results, are shown in Fig. 8 (b) and provides an increase in performance at a TSR value that is almost the same, namely 30.77% from the previous result [28] and 18.9% from previous study [32]. For experimental results, an increase of 7.14% was obtained from the previous experimental results [28].

Table 4 Test Data LED

| Test Data with Lighting light | | |
|-------------------------------|-----------------------------|---------------------------|
| Load | Current, I , out (Ampere) | Voltage, V , out (Volt) |
| LED light | 2.5 | 12 |

Table 5 Calculation Result Data

| Wind speed (m/s) | Force, F (N) | Torque, T (Nm) | VAWT rotation (rpm) | Angular velocity, ω (rad/s) | Wind power (Watt) | VAWT power (Watt) | Electric power (Watt) |
|------------------|----------------|------------------|---------------------|------------------------------------|-------------------|-------------------|-----------------------|
| 1.16 | 2.07 | 0.41 | 57.6 | 6.03 | 1.20 | 2.50 | 0.39 |
| 2.6 | 10.40 | 2.08 | 110.9 | 11.61 | 13.52 | 24.15 | 1.34 |
| 2.71 | 11.30 | 2.26 | 147.6 | 15.45 | 15.31 | 34.92 | 1.60 |
| 2.79 | 11.98 | 2.40 | 143.9 | 15.07 | 16.71 | 36.10 | 2.58 |
| 3.2 | 15.76 | 3.15 | 179.4 | 18.78 | 25.21 | 59.18 | 2.24 |

Table 6 C_p comparison of numerical and experimental

| NUMERICAL | | EXPERIMENTAL | |
|------------|--------------|--------------|--------------|
| TSR = 1.0 | $C_p = 0.24$ | TSR = 1.11 | $C_p = 0.14$ |
| TSR = 1.12 | $C_p = 0.20$ | TSR = 1.28 | $C_p = 0.13$ |



Fig. 7 (a) VAWT current study after assembly; and (b) VAWT test at night

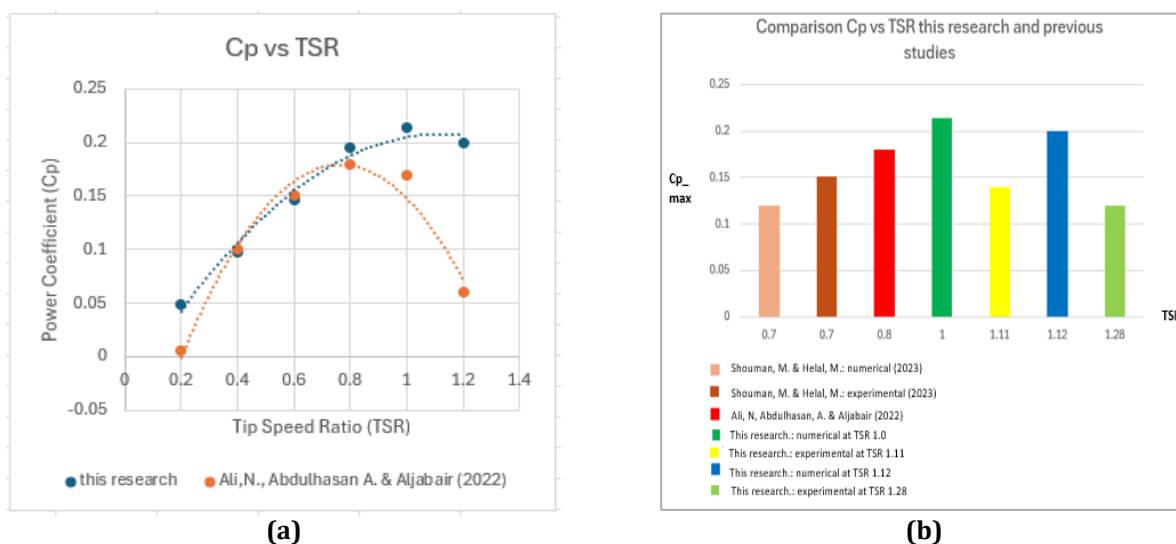


Fig. 8 (a) Comparison this research with conventional; and (b) Comparison C_p -max this research with previous studies

5. Conclusions

From the numerical result, the flow pattern that occurs around the turbine suggests that the design of the tapered blade has a more diffused pattern of spinning than conventional blade, and the turbulence occurring at the TSR = 1.0 is still in the turbine sweep area. The experimental test results indicate that maximum efficiency is achieved when the wind intensity is constant, so that it can produce large voltages and currents. VAWT can still rotate at a low wind speed of less than 1 m/s, but cannot charge the accumulator. From Table VI, on the TSR relatively the same, the difference between C_p of numerical and experimental results is about 50.1%. This is reasonable because

the experiments included loads, lights, generators, and so on. The generator can only charge the battery at a minimum wind speed of 2 m/s, and based on the test results, VAWT can provide electricity for lighting for 4 hours. So, the target of this research has been achieved. It is seen that the Savonius type VAWT can function properly and can produce electrical power so that it can be used as a source of street lighting. Further research, the installation of wind turbines as a result of this study will be hybridized with solar cells so that they can be used to work throughout the season in Indonesia.

Acknowledgement

This research was made possible through monetary assistance by Pusat Penelitian dan Pengabdian Masyarakat Politeknik Negeri Bandung.

Conflict of Interest

Authors declare that there is no conflict of interests regarding the publication of the paper.

Author Contribution

*The authors confirm contribution to the paper as follows: Maria **study conception and design, numerical calculation, and supervised the finding of the results**; Yackob, Maria and Singgih, **data collection, analysis and interpretation of numerical results**; M. Rizki, M.Luthfi, and Syaiful **fabricated the prototype of wind turbine including mechanical and electrical components**, **supervised by Maria**; Maria, Singgih, M. Zuhri, and Yackob carried out the prototype experimen. Maria took the lead in **writing the article manuscript**. All authors reviewed the results and provided critical feedback and helped shape the research, analysis and manuscript.*

References

- [1] Enerdata, "Indonesia Energy Information," 2021. [Online]. Available: <https://www.enerdata.net/estore/energy-market/indonesia>
- [2] L. Sanchez and B. Luan, "The Health Cost of Coal in Indonesia," GSI Report, Geneva, 2018. <https://www.iisd.org/system/files/publications/health-cost-coal-indonesia.pdf>
- [3] H. Sasana, F. Salman, Suharmono, S. B. M. Nugroho and A. G. E. Yusuf, "Sasana, H. et al., "The Impact of Fossil Energy Subsidies on Social Cost in Indonesia", IJEEP, vol. 8, no. 2, pp. 168–173, .," International Journal of Energy Economics and Policy, p. 168–173, 2018. <https://www.econjournals.com/index.php/ijeep/article/view/6162>
- [4] FINAL SESA SCOPING REPORT, "Strategic Environmental and Social Assessment (SESA) of the Energy Transition Mechanism (ETM) in Indonesia," Ciera Group and PT Hatfield Indonesia, 2003. https://fiskal.kemenkeu.go.id/docs/SESA_Scoping_Report_EN.pdf
- [5] ecologi, "Sidrap Windfarm Indonesia," 2023. [Online]. Available: <https://ecologi.com/projects/sidrap-wind-farm-indonesia>.
- [6] Erwin, T. P. Soemardi, A. Surjosatyo, J. Nugroho, K. Nugraha and S. Wiyono, "Design optimization of hybrid biomass and wind turbine for minapolitan cluster in Domas, Serang, Banten, Indonesia," in IOP Conference Series: Earth and Environmental Science, 2018. <https://doi.org/10.1088/1755-1315/105/1/012010>
- [7] A. Hajramurni, Second Sulawesi wind farm project near completion, Jakarta: The Jakarta Post, 2018. <https://www.thejakartapost.com/news/2018/11/07/second-sulawesi-wind-farm-project-near-completion.html>
- [8] Dirjen EBTKE, "Potensi Energi Angin Indonesia 2020," January 2021. [Online]. Available: https://p3tkebt.esdm.go.id/pilot-plan-project/energi_angin/potensi-energi-angin-indonesia-2020.
- [9] H. D. Puspitarini, "Beyond 443 GW: Indonesia's infinite renewable energy potentials," October 2021. [Online]. Available: <https://iesr.or.id/en/pustaka/beyond-443-gw-indonesias-infinite-renewableenergy-potentials>.
- [10] L. Noviani, "Assessment of the Wind Power Application in Indonesia," Indonesian Journal of Physics and Nuclear Applications, pp. 78-85, 2019. [ginermaslebu,+Journal+editor,+p78_85_3729-Article+Text-14707-1-2-20200703+\(FIX\) \(7\).pdf](https://doi.org/10.33116/ije.v2i2.37)
- [11] D. L. Priandaru and N. A. Pambudi, "Wind Energy in Indonesia: Current Status, Potential, Challenge, Opportunities, and Future Policy," Indonesian Journal of Energy, p. 65 – 73, 2019. <https://doi.org/10.33116/ije.v2i2.37>
- [12] U. K. Saha, S. Thotla and D. Maity, "Optimum design configuration of Savonius rotor through wind tunnel experiments," Journal of Wind Engineering and Industrial Aerodynamics, p. 1359–1375, 2008. <https://doi.org/10.1016/j.jweia.2008.03.005>

- [13] J. Su, Y. Chen, Z. Han, D. Zhou, Y. Bao and Y. Zhao, "Investigation of V-shaped blade for the performance improvement of vertical axis wind turbines," *Applied Energy*, Elsevier, vol 260(C), 2020. <https://ideas.repec.org/a/eee/appene/v260y2020ics0306261919320136.html>
- [14] C. Stout, S. Islam, A. White, S. Arnott, E. Kollovozi, M. Shaw, G. Droubi, Y. Sinha and B. Bird, "Efficiency Improvement of Vertical Axis Wind Turbines with an Upstream Deflector," *Energy Procedia*, pp. 141-148, 2017. <https://doi.org/10.1016/j.egypro.2017.07.032>
- [15] J. Yen and N. Ahmed, "Improving safety and performance of small-scale vertical axis wind turbines," *Procedia Engineering*, p. 99-106, 2012. <https://doi.org/10.1016/j.proeng.2012.10.117>
- [16] J.-L. Menet and T. d. Rezende, "Static and dynamic study of a conventional Savonius rotor using a numerical simulation," in *CFM 2013- 21ème Congrès Français de Mécanique*, Bordeaux, 2013. <https://hal.science/hal-01078076/document>
- [17] A. Sanusi, S. Soeparman, S. Wahyudi and L. Yuliaty, "Experimental Study of Combined Blade Savonius Wind Turbine," *International Journal of Renewable Energy Research-IJRER*, pp. 614-619, 2016. https://www.researchgate.net/publication/305416408_Experimental_study_of_combined_blade_savonius_wind_turbine
- [18] A. Nemati, "Three-dimensional numerical study of the performance of a small combined Savonius-Darrieus vertical wind turbine," *Iranian Journal of Energy and Environment*, p. 163-169, 2020. <https://doi.org/10.5829/ijee.2020.11.02.11>
- [19] A. Pallotta, D. Pietrogiacomi and G. P. Romano, "HYBRI – A combined Savonius-Darrieus wind turbine: Performances and flow fields," *Energy*, 2020. <https://doi.org/10.1016/j.energy.2019.116433>
- [20] J. Lee and F. Zhao, "Global wind report 2021," *Global Wind Energy Council (GWEC)*, Brussel, Belgium, 2021. <https://gwec.net/wp-content/uploads/2021/03/GWEC-Global-Wind-Report-2021.pdf>
- [21] N. Mishra, A. Jain, A. Nair, B. Khanna and S. Mitra, "Numerical and experimental investigations on a dimpled savonius vertical axis wind turbine," *IJRER*, p. 646-653, 2020. <https://doi.org/10.20508/ijrer.v10i2.10566.g7935>
- [22] H. Belmili, R. Cheikh, T. Smail, N. Seddaoui and R. Biara, "Study, design and manufacturing of hybrid vertical axis Savonius wind turbine for urban architecture," *Energy Procedia*, pp. 330-335, 2017. <https://doi.org/10.1016/j.egypro.2017.10.389>
- [23] A. Al-Faruk and A. Sharifian, "Flow Field and Performance Study of Vertical Axis Savonius Type SST Wind Turbine," *Energy Procedia*, pp. 235-242, 2017. DOI: 10.1016/j.egypro.2017.03.133
- [24] M. Zemamou, M. Aggour and A. Toumi, "Review of savonius wind turbine design and Performance," *Energy Procedia*, pp. 383-388, 2017. <https://doi.org/10.1016/j.egypro.2017.11.047>
- [25] B. Altan and G. S. Gultekin, "Investigation of Performance Enhancements of Savonius Wind Turbines through Additional Designs," *Processes*, 2023, Vol. 11, No. 5, 1473, May 2023. <https://doi.org/10.3390/pr11051473>
- [26] B. Deda Altan and A. Gungor, "Investigation of the turbine performances in the case of dual usage of Savonius wind turbines," in *Proc. Inst. Mech. Eng. Part E J. Proc. Mech. Eng.*, 2022. <https://doi.org/10.1177/0954408922140217>
- [27] C. Promdee and C. Photong, "Effects of wind angles and wind speeds on voltage generation of Savonius wind turbine with double wind tunnels," *Procedia Computer Science*, p. 401-404, 2016. <https://doi.org/10.1016/j.procs.2016.05.044>
- [28] M. Shouman, M. Helal and A. El-Haroun, "Numerical prediction of improvement of a Savonius rotor performance with curtaining and fin addition on blade," *Alexandria Engineering Journal*, p. 10689-10699, 2022. <https://doi.org/10.1016/j.aej.2022.03.079>
- [29] S. Sridhar, J. Joseph and J. Radhakrishnan, "Implementation of tubercles on Vertical Axis Wind Turbines (VAWTs): An Aerodynamic Perspective," *Energy Technol. Assess*, p. 2022. <https://doi.org/10.1016/j.seta.2022.102109>
- [30] Č. Kostić, "Review of the Spalart-Allmaras Turbulence Model and its Modifications to Three-Dimensional Supersonic Configurations," *Scientific Technical Review*, pp. 43-49, 2015. <https://scindeks-clanci.ceon.rs/data/pdf/1820-0206/2015/1820-02061501043K.pdf>
- [31] ANSYS, "Spallart-Almaras Model, Transport Equation for the Spalart-Allmaras Mode," 2024. [Online]. Available: <https://www.afs.enea.it/project/neptunius/docs/fluent/html/th/node50.html>.
- [32] N. Ali, A. Abdulhasan and S. Aljabair, "Aerodynamic Performance of Vertical and Horizontal AXIS Wind Turbines: A Comparison Review," *IJOST*, 2022. : <https://doi.org/10.17509/ijost.v7i1>